Journal of Engineering Mathematics **44:** 107–123, 2002.

Control over electric field in traveling wave applicators

KONSTANTIN A. LURIE and VADIM V. YAKOVLEV
Department of Mathematical Sciences, Worcester Polytechnic Institute, Worcester, MA 01602, U.S.A.
e-mail: vadim@wpi.edu

Received 21 November 2001; accepted in revised form 3 June 2002

Abstract. A method of optimal material design is applied to the problem of controlling the distribution of the electric field within a material heated by microwaves in closed cavities. Analytical and computational procedures are presented for a layer in a single-mode rectangular waveguide applicator. These determine the optimal placing and micro-geometry of composite controlling materials. The particular case of a lossless layer is illustrated numerically: it is shown that the controlling material becomes uniform with a dielectric constant which always exceeds the layer to be heated.

Key words: composite materials, lossless material, microwave heating, optimization, waveguide

1. Introduction

Microwave heating is known to be a unique technique of volumetric thermal processing of dielectric materials [1, 2]. In many cases, a uniform temperature distribution within the product is required, and the literature on microwave processing suggests various means to achieve an even pattern of heat release.

Mechanical devices like stirrers and turntables provide an empirical solution to the problem in its non-deterministic setup. The multiple modes are thoroughly mixed to achieve a random field distribution and therefore to increase the probability of uniform heat release. Among other methods working on “statistical" principles, there should be mentioned active packaging [3], monitoring of the microwave power level [4], the variable frequency [5], and the multiple input of energy [1, 6]. Despite evident attractive features, the practical implementation of these methods showed the lack of uniformity in a number of important cases. These methods do not provide an effective control adapted to a specific material, and are based on a purely intuitive expectation that the diversity of participating modes will secure the uniformity of heat release in space-time.

There have also been attempts to improve the temperature patterns generated by a single mode. In [7, 8], there was considered a possibility of creating the uniform field by formation of the TEM mode in a rectangular waveguide partially filled with dielectric slabs; a similar technique was used in [9] for a resonant cavity. Such approaches have not, however, included a realistic means to eliminate the higher modes that may well emerge once the operating chamber is filled with a processed material. For this reason in particular, the TEM mode has a practical implementation only in applications related to irradiation [10].

The supplementary metal ridges [11] and grids [12], the mechanical change of the chamber’s size [13], and the use of evanescent modes [14] are among other means used to correct fields generated by deterministic modes. All these efforts are insufficient because the geometry of material inclusions as well as their deployment throughout the operating chamber are

motivated by engineering experience alone, both theoretical and experimental. In spite of its obvious merits, this experience is limited, and it therefore fails to exhause completely the possibilities of improvement intrinsic in the system itself.

In order to derive new methods for creating uniform fields, a rigorous mathematical approach is necessary. Sophisticated computer modeling [15–18] based on numerical discretization may be efficient for the analysis, but it cannot give direct recommendations as to how the system should be changed to guarantee improvement of the temperature distribution within the product. The need to apply some kind of optimization to arrange more effective processing was recognized in [19]. Straightforward computer optimization incorporating complete numerical solution of the electromagnetic problems still appears to be too time-consuming. For this reason, the authors dealing with optimization of microwave heating restricted themselves to some faster and simpler computational kernels, such as methods of moments [17], or models bypassing Maxwell's equations alltogether [20].

The present paper suggests an effective way to put the temperature distribution under direct control. The required formalization emerges from the idea of optimal material design (OMD) [21]. In the context of microwave thermal processing, the goal of OMD is to find an optimal placing of supplementary dielectric materials within a part of the operating chamber in order to focus the electromagnetic field appropriately onto the heated product to maintain the desired (*e.g.*, uniform) heat release within the processed material. Control over the material properties implemented locally produces a substantially stronger influence upon the electromagnetic field than control over the distribution of the electromagnetic power supplied directly from generator [20] or over the field pattern in the structures with the optimized boundary shape [22, 23].

Unlike computer optimization, this approach allows one to avoid multiple numerical solution in a computational "cycle", but from the beginning offers the optimality conditions that characterize the desired solution. In contrast to attempts to enhance the electric field uniformity by using dielectric slabs partially filling the operating chambers [7–9, 24, 25], the location, structure, and permittivity of a focusing material are determined by the OMD method. They are found, not empirically but rigorously, as the means guaranteeing the required heat release. The homogenization method relevant to optimal material design has been used for optimization of magnetic devices at low frequencies in [26]. The OMD principles are applied for the first time to the problem of the control of high frequency electromagnetic fields.

2. Background

In general, microwave heating is a very complicated process depending on many physical parameters. The processed material may have non-uniform composition, non-smooth configuration, and temperature-dependent complex permittivity. The heating chambers differ in geometry, type of field excitation, the placement (orientation) of the product, etc. The problem of control of microwave heating becomes hard to formalize in such a general setting. Therefore, we narrow the problem and concentrate on fully deterministic, non-random processes. Specifically, we assume that:

i. the processed samples may have arbitrarily complex composition, but the distribution of their material properties is well determined;

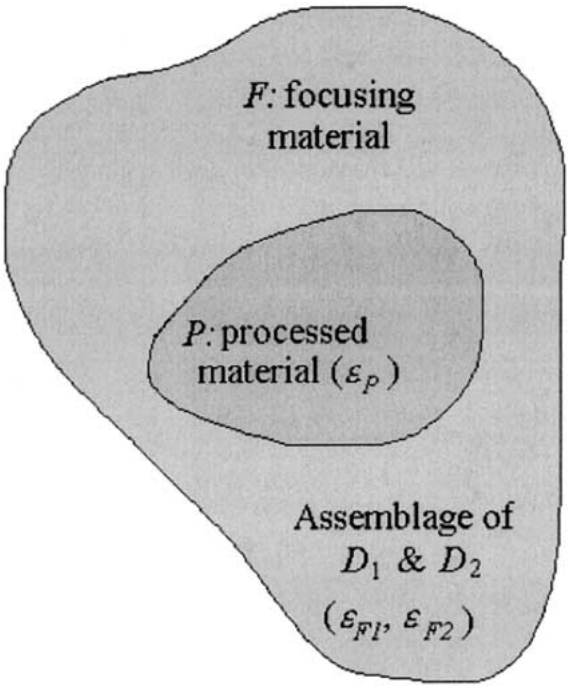

Figure 1. Closed microwave heating cavity: focusing structure and heated material.

ii. the shape of the samples is known, that is, the boundary conditions can be adequately posed;
iii. a finite number of propagating modes is allowed to be subject to deterministic control.

With these assumptions it is possible to cover many practically significant situations. In order to demonstrate the capabilities of optimal material design in controlling of microwave heating, we further specify the problem and consider waveguide systems that appear to be the most suitable for setting the deterministic wave patterns.

The OMD concept says that the field focusing can be successfully implemented with the aid of an assemblage of two dielectric materials D_1 and D_2 differing in their permittivities and appropriately distributed within some part F of an operating chamber embracing the heating zone P occupied by the processed sample (Figure 1). The layout of these materials serves as the key factor controlling the spatial distribution of the field, and, consequently, the heat release within P. Finding this layout is the main goal of the approach.

We are looking for the disposition of the focusing materials in F capable of minimizing the difference between the acting heat release $q(x, t)$ within P and some desired distribution $q_0(x, t)$. Such a difference becomes the cost (objective) functional; as an example, one may consider the mean square difference between the two distributions:

$$I = \int_0^{t_1} \int_P |q(x, t) - q_0(x, t)|^2 \mathrm{d}x\mathrm{d}t, \tag{1}$$

where t_1 denotes the period of heating. This functional combines both spatial and temporal variations of the field and may be equally applied in the presence and/or absence of the temperature dependence of the product's permittivity. Along with (1), other types of cost functionals, *e.g.*, linear functionals, may be introduced.

The goal of design is to minimize the functional by an appropriate layout of D_1 and D_2 in F. The field distribution within F and P is governed by the field equations and the relevant boundary conditions. The presence of such constraints is the key factor that distinguishes problems of optimal material design from traditional variational problems of minimization of functionals. In other words, the quantity q in (1) should be chosen not among the functions possessing just conventional smoothness properties, but it should rather be sought among solutions to a side boundary-value problem depending upon control. The search for an optimal $q(x, t)$ therefore reduces to the search for optimal control. The complexity of this problem is due to the implicit influence produced by a control upon the heat release: this influence comes through the boundary-value problem and is not reflected directly in the functional through its explicit dependence upon control. Such a concept is different from the approach addressed in many publications (*e.g.*, [22, 27]) where the functional appears to be explicitly control-dependent.

The typical optimal layouts possess one common feature: certain parts of F (or the whole of it), become occupied by *composites* assembled from D_1 and D_2 [21]. Composites are formations assembled from original materials distributed on a spatial microscale. The relevant microgeometries may vary; in particular, we shall consider alternating layers of two different materials forming a laminate structure. The width of the layers should be chosen small compared to the wavelength. The appearance of composites is crucial: they appropriately redistribute the electromagnetic field everywhere, particularly in P, to the final effect of minimization of the cost functional (1).

In our problem, Maxwell's equations are solved for domains F and P under suitable boundary conditions. Controls (permittivities of the focusing structure) are distributed throughout F, whereas the heat release to be controlled is distributed over P. Material properties of the substance within P are assumed given. The heat release generates the temperature pattern within the product according to the heat equation.

The domain F is occupied by two dielectrics D_1 and D_2 with different permittivities ϵ_1 and ϵ_2; we look for their layout in F that finally makes the distribution of temperature within the domain P as close as possible to the desired pattern. This influence is implemented through the direct effect produced by a non-uniform dielectric material in F upon the field distribution, and consequently, the heat release within P.

Since the heat release is proportional to the imaginary part of complex permittivity and the squared magnitude of the electric field, the control of microwave heating can be eventually implemented through the control of the electric field. In this paper, we are interested in evening up the electric field of the dominant mode in a dielectric layer in a rectangular waveguide. However, a conceptually similar approach could be used to obtain uniform or other desirable field distributions in the processed material of other configurations.

3. Analysis

Consider a rectangular TE_{10} applicator with sides a and b. The material to be processed is assumed to be a uniform layer with permittivity $\epsilon_p = \epsilon_p' - i\epsilon_p''$ and permeability $\mu = 1$; it occupies domain $P(x \in [x_1, x_2], 0 < x_1 < x_2 < a, y \in [0, b])$ of the cross-section of the waveguide (Figure 2).

Generally, the dielectric filling generates conditions for propagation of both dominant and higher modes. Any change in the filling's parameters (permittivities or/and geometry) may

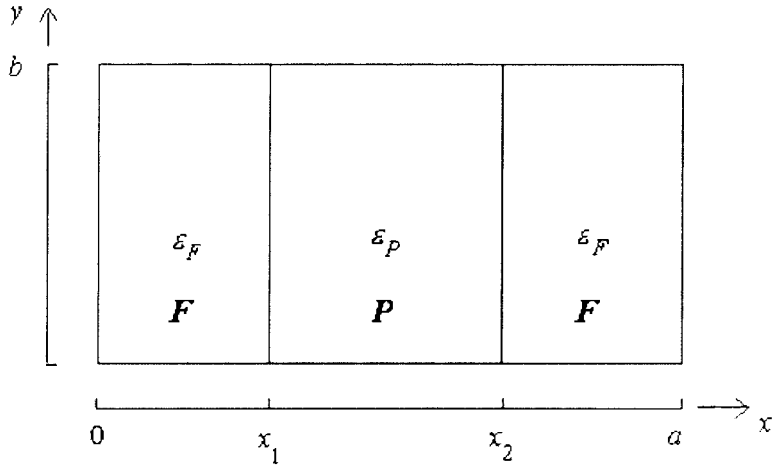

Figure 2. Cross-section of a rectangular traveling wave applicator with focusing (F) and processed (P) materials.

affect the number of propagating modes, and this influence should be taken into consideration, particularly, when we optimize parameters of the focusing structure. The electric field in P is known to be a superposition of propagating modes, and to make this field uniform we have to apply a sophisticated composite layout aimed to even up these combined modes. It seems to be reasonable to develop a simplified analysis for a single (dominant) mode. This can be achieved, for example, by an appropriate change of the waveguide's dimensions preserving, however, the material filling pattern. For the higher modes, it would be possible to generate a similar analysis following the scheme available for the dominant mode.

To specify the starting points, we notice that the orientation of electric and magnetic vectors in the dominant mode replicates the orientation of these vectors in the TE_{10} mode in an empty waveguide: they are parallel to the y- and x-axes, respectively. In these circumstances, the general method shows that the material layout that will not destroy the above orientation of the field vectors may only be a lamination with the layers along the y-axis. A uniform dielectric represents a special case of lamellar layout.

Therefore, our goal is to locate controlling dielectric materials in two lateral domains F : ($0 < x < x_1, 0 < y < b$, and $x_2 < x < a, 0 < y < b$), in such a way as to obtain a uniform distribution of the electric field of the dominant mode within P.

The electric field has only a y-component

$$E_y(x) = u(x)\mathrm{e}^{-\mathrm{i}\gamma z}, \tag{2}$$

where $u(x)$ is the complex magnitude, $\gamma = \beta - \mathrm{i}\alpha$ is the propagation factor, β is the phase constant, and α is the attenuation constant. The magnitude u satisfies the Helmholtz's equation

$$u''(x) + h(x)u(x) = 0 \tag{3}$$

with $u = v - \mathrm{i}w$, $h = \omega^2\epsilon - \gamma^2 = f - \mathrm{i}g$, where ω is circular frequency. In (3), ϵ is defined as

$$\epsilon(x) = \begin{cases} \epsilon_{F1}, \text{ or } \epsilon_{F2}, & \text{for } x \in (0, x_1), \\ \epsilon_P, & \text{for } x \in (x_1, x_2), \\ \epsilon_{F1}, \text{ or } \epsilon_{F2}, & \text{for } x \in (x_2, a). \end{cases} \tag{4}$$

For the TE_{10} mode, the following boundary conditions hold:

$$\begin{aligned} u(0) &= 0, \\ u(x_1)|_-^+ &= 0, \quad u'(x_1)|_-^+ = 0, \\ u(x_2)|_-^+ &= 0, \quad u'(x_2)|_-^+ = 0, \\ u(a) &= 0. \end{aligned} \tag{5}$$

Within the processed material, we require the uniform field:

$$u(x) = 1; \quad x \in (x_1, x_2). \tag{6}$$

This means that the minimal requirement for the functional (1) might be expressed as:

$$\int_{x_1}^{x_2} [u(x) - 1]^2 \mathrm{d}x \to \min. \tag{7}$$

Assume that requirement (6) is satisfied by a uniform controlling material F. Then we apply (2) to the processed material, where the field u is assumed constant. Since $u'' = 0$, we conclude that $h = 0$ in P, *i.e.*

$$\omega^2 \epsilon'_P = \beta^2 - \alpha^2, \quad \omega^2 \epsilon''_P = 2\alpha\beta. \tag{8}$$

Then, in the domain F,

$$u = A \cos \sqrt{h} x + B \sin \sqrt{h} x \tag{9}$$

is the solution to (2). Given the boundary condition $u(0) = 0$, we obtain that $A = 0$. Because of (6) and the continuity of u' across the points x_1 and x_2, we conclude that

$$\cos \sqrt{h} x_1 = 0, \quad \sqrt{h} = \frac{\pi}{2x_1}, \tag{10}$$

and, therefore, $\Im \mathrm{m} h = 0$ within F. By virtue of (8), this means that $\omega^2 \epsilon'' = 2\alpha\beta$, and (9) now shows that $\epsilon''_F = \epsilon''_P$. Thus, the field within P may become uniform only provided that the controlling material possesses the same losses as the processed one, at least provided that the material is uniform, as we assumed above.

Therefore, we arrive at the following two options. We may allow for the absorbing controlling material, and thus secure the field uniformity in the processed layer. Alternatively, we may admit some non-uniformity of the field within the processed material by preserving the controlling material lossless (or possessing negligible losses) and at the same time being non-uniform. The latter option appears to be preferable because otherwise we would agree on substantial heating of the controlling materials which would be practically unfeasible. The non-uniformity of the focusing structure thus becomes a decisive factor affecting the degree of non-uniformity of the field within the processed material.

Because of the symmetry with respect to the mid-line $x = a/2$, we consider the left half of the waveguide cross-section (Figure 3). Specifically, we assume that there are two materials D_1 and D_2 in F with $\epsilon_{F1} = \epsilon'_{F1} - i\epsilon''_{F1}$ and $\epsilon_{F2} = \epsilon'_{F2} - i\epsilon''_{F2}$ that alternate in vertical layers. The average quantities

$$f = mf_1 + (1 - m) f_2, \quad g = mg_1 + (1 - m) g_2 \tag{11}$$

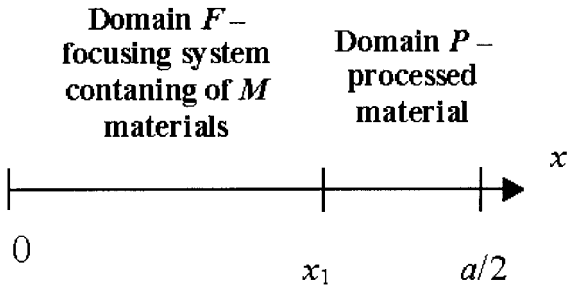

Figure 3. Two domains in the symmetric half-interval for the applicator in Figure 2.

are introduced, where m denotes the volume fraction of D_1 with f_1 and g_1 in the lamination assemblage. The average quantities

$$v = mv_1 + (1-m)v_2, \quad w = mw_1 + (1-m)w_2 \tag{12}$$

satisfy Equation (3) with $h = f - \mathrm{i}g = m_1h_1 + (1-m)h_2$, and it becomes:

$$v'' + fv - gw - \mathrm{i}(w'' + fw + gv) = 0. \tag{13}$$

This complex second-order equation can be rewritten as the equivalent first order system

$$\begin{cases} v' = p, \\ p' = -fv + gw, \\ w' = q, \\ q' = -gv - fw \end{cases} \tag{14}$$

by introduction of the auxiliary variables p, q. In the domain F, the right-hand sides of these equations depend by (11) on the volume fraction $m = m(x)$ that serves as the control subject to the inequalities

$$0 \le m(x) \le 1. \tag{15}$$

The field in the domain P is governed by the system (14) in which f and g take the constant values f_P and g_P, respectively, specified for the processed material. In the domain F, f and g are specified by the materials in the lamination assemblage, that is:

$$\begin{aligned} f_P &= \omega^2\epsilon'_P + \alpha^2 - \beta^2, \quad g_P = \omega^2\epsilon''_P - 2\alpha\beta, \\ f_{Fi} &+ \omega^2\epsilon'_{Fi} + \alpha^2 - \beta^2, \quad g_{Fi} = \omega^2\epsilon''_{Fi} - 2\alpha\beta, \quad i = 1, 2. \end{aligned} \tag{16}$$

For any fixed control $m(x)$, we look for the solution $\{v(x), p(x), w(x), q(x)\}$ of (14) for both F and P, satisfying boundary conditions (5) which can now be rewritten as:

$$\begin{aligned} v(0) &= w(0) = 0, \\ v(x_1)|_-^+ &= w(x_1)|_-^+ = p(x_1)|_-^+ = q(x_1)|_-^+ = 0, \\ p(a/2) &= q(a/2) = 0. \end{aligned} \tag{17}$$

Optimization means finding the control $m(x)$ subject to constraints (15) that minimizes the functional (7) which can be expressed now as follows:

$$I = \int_{x_1}^{a/2} \left(\sqrt{v^2 + w^2} - 1\right)^2 \mathrm{d}x. \tag{18}$$

This functional characterizes the deviation (in the L_2-norm) of the magnitude of the field from the constant value 1 in the domain P occupied by the processed material. Following the standard procedure of the theory of optimal design [21], we construct the Hamiltonian H with the aid of the conjugate variables (Lagrange multipliers) V, P, W, Q, and the factor $\rho = \rho(x)$ defined as 0 within F and 1 within P. The conjugate variables should satisfy the system:

$$\begin{cases} V' = \dfrac{2\rho v}{\sqrt{v^2 + w^2}} \left(\sqrt{v^2 + w^2} - 1\right) + fP + gQ \\ P' = -V \\ W' = \dfrac{2\rho w}{\sqrt{v^2 + w^2}} \left(\sqrt{v^2 + w^2} - 1\right) - gP + fQ \\ Q' = -W \end{cases} \tag{19}$$

along with the boundary conditions:

$$\begin{aligned} P(0) &= Q(0) = 0, \\ V(x_1)|_-^+ &= W(x_1)|_-^+ = P(x_1)|_-^+ = Q(x_1)|_-^+ = 0, \\ V(a/2) &= W(a/2) = 0. \end{aligned} \tag{20}$$

The expression for H takes the following form:

$$H = -\rho(v^2 + w^2 - 1) + pV - (vP + wQ) f_{F2} + (wP - vQ) g_{F2} + mH_1 \tag{21}$$

with

$$H_1 = -(vP + wQ)\Delta f_F + (wP - vQ)\Delta g_F, \tag{22}$$

where

$$\Delta f_F = f_{F1} - f_{F2}; \quad \Delta g_F = g_{F1} - g_{F_2}. \tag{23}$$

The necessary condition of optimality [21] now indicates that there may be three ranges for m given by:

i. If $H_1 < 0$, then $m = 0$, and F is occupied by material D_2.

ii. If $H_1 > 0$, then $m = 1$, and F is occupied by material D_1.

iii. If $H_1 = 0$, the *singular range* takes place.

Additional analysis shows that in the singular range, the volume fraction $m(x)$ is calculated analytically as a special combination of the original and conjugate variables and the material parameters:

$$m = \frac{\rho(v^2 + w^2)\Delta f_F + (Vp + Wq)\Delta f_F - (Vq - Wp)\Delta g_F}{(Pv + Qw)[(\Delta f_F)^2 + (\Delta g_F)^2]} - \frac{g_2}{\Delta g_F}. \tag{24}$$

The option (i) shows that at those parts of F, where $H_1 < 0$, material D_2 alone should be applied; at those parts where $H_1 > 0$, there should be placed D_1 alone. If, however, $H_1 = 0$ at some part of F, then these parts should be occupied by a layered composite assembled from

D_1 and D_2 taken, respectively, with the volume fractions m and $(1-m)$. So the behavior of H_1 on F specifies the micro-geometry of the focusing system.

Similar analysis could be performed for more than two materials in F as well as for the higher modes with the same orientation of the field vectors (TE_{20}, TE_{30}, etc.). For other modes, alternative material layout (different from the lamination along the y-axis) may produce better control. To find out the orientation of the electric field vector in those modes and to choose an appropriate structure of the focusing material, relevant numerical analysis can be applied.

4. Computation

The approach described above can be implemented as follows. The systems (14) and (19) can be solved independently. We start with (14) and rewrite it in the form:

$$\mathbf{u}' = \mathbf{A}_{F,P}\mathbf{u} \quad \text{with} \quad \mathbf{A}_F \quad \text{for} \quad x \in (0, x_1) \quad \text{and} \quad \mathbf{A}_P \quad \text{for} \quad x \in (x_1, a/2), \tag{25}$$

where $\mathbf{A}_{F,P}$ denote matrices depending on $f_{F1,2}$, $g_{F1,2}$ and f_P, g_P, respectively (see Appendix), and $\mathbf{u} = [v \quad p \quad w \quad q]^T$. Seeking the solution in the form $y = e^{\lambda_{F,P}x}\xi$, we reduce (25) to the eigenvalue problem:

$$\mathbf{A}_{F,P}\xi_{F,P} = \lambda_{F,P}\xi_{F,P}, \tag{26}$$

with four eigenvalues at each subinterval $0 \le x \le x_1$ and $x_1 \le x \le \frac{a}{2}$. Therefore, the general solution to (14) may be represented as the linear combinations:

$$\mathbf{y}_{F,P} = \begin{bmatrix} e^{\lambda^{(1)}_{F,P}x}\xi^{(1)}_{F1,P1} & \dots & e^{\lambda^{(4)}_{F,P}x}\xi^{(4)}_{F1,P1} \\ \vdots & \dots & \vdots \\ e^{\lambda^{(1)}_{F,P}x}\xi^{(1)}_{F4,P4} & \dots & e^{\lambda^{(4)}_{F,P}x}\xi^{(4)}_{F4,P4} \end{bmatrix} \begin{bmatrix} C^{(1)}_{F,P} \\ \vdots \\ C^{(4)}_{F,P} \end{bmatrix}. \tag{27}$$

By (27), the system of the boundary conditions (17) may be presented in the matrix form:

$$\mathbf{BC} = 0, \tag{28}$$

where $\mathbf{B}$ is the 8×8-matrix given in Appendix and $\mathbf{C}$ is the vector of unknown constants (four in F and four in P). Equation (28) possesses non-trivial solutions if $\det\mathbf{B} = 0$.

Upon finding the eight constants, we determine the variables $\{v \quad p \quad w \quad q\}$ and then these can be inserted into (19) which, in its turn, can be solved with respect to the conjugate variables $\{V \quad P \quad W \quad Q\}$. System (19) can be rewritten in the matrix form:

$$\begin{cases} \mathbf{U}' = \mathbf{D}_F\mathbf{U}; & \text{for} \quad x \in (0, x_1) \quad \text{(a)} \\ \mathbf{U}' = \mathbf{D}_P\mathbf{U} + \mathbf{F}; & \text{for} \quad x \in (x_1, a/2) \quad \text{(b)}, \end{cases} \tag{29}$$

where $\mathbf{D}_F$ and $\mathbf{D}_P$ are matrices depending on $f_{F1,2}$, $g_{F1,2}$ and f_P, g_P, respectively (see Appendix), and $\mathbf{U} = [V \quad P \quad W \quad Q]^T$, and

$$\mathbf{F} = \begin{bmatrix} Gv \\ 0 \\ Gw \\ 0 \end{bmatrix}; \quad G = \frac{2}{\sqrt{v^2 + w^2}}\left(\sqrt{v^2 + w^2} - 1\right). \tag{30}$$

Since the solution of (29a) can be found in the form $z_F = \mathrm{e}^{\bar{\lambda}_F x}\bar{\xi}_F$, this matrix equation is equivalent to the eigenvalue problem:

$$\mathbf{D}_F\bar{\boldsymbol{\xi}}_F = \bar{\lambda}_F\bar{\boldsymbol{\xi}}_F, \tag{31}$$

which holds for the domain occupied by the focusing system F. It provides four eigenvalues defined at $[0, x_1)$. So the general solution to (29a) may be represented as the linear combination:

$$\mathbf{Z}_F = \begin{bmatrix} \mathrm{e}^{\bar{\lambda}_F^{(1)}x}\bar{\xi}_{F1}^{(1)} & \dots & \mathrm{e}^{\bar{\lambda}_F^{(4)}x}\bar{\xi}_{F1}^{(4)} \\ \vdots & \dots & \vdots \\ \mathrm{e}^{\bar{\lambda}_F^{(1)}x}\bar{\xi}_{F4}^{(1)} & \dots & \mathrm{e}^{\bar{\lambda}_F^{(4)}x}\bar{\xi}_{F4}^{(4)} \end{bmatrix} \begin{bmatrix} \bar{C}_F^{(1)} \\ \vdots \\ \bar{C}_F^{(4)} \end{bmatrix}, \tag{32}$$

where $\bar{\mathbf{C}}_F$ is the vector of constants specified by the boundary conditions.

The general solution of (29b) may be found assuming that the fundamental solution is known for the corresponding homogeneous system

$$\mathbf{U}' = \mathbf{D}_P\mathbf{U}. \tag{33}$$

The solution of (29a) can also be found in the form $z_{Ph} = \mathrm{e}^{\bar{\lambda}_{Ph}x}\bar{\xi}_{Ph}$, and thus (33) is equivalent to the eignevalue problem

$$\mathbf{D}_P\bar{\boldsymbol{\xi}}_P^{(g)} = \bar{\lambda}_P^{(g)}\bar{\boldsymbol{\xi}}_P^{(g)}, \tag{34}$$

which holds for the domain occupied by the processed material P and has four eigenvalues in the interval $(x_1, a/2]$. The general solution to the last equation can be expressed as:

$$\begin{aligned} \mathbf{z}_P^{(g)}(x) &= \begin{bmatrix} \mathrm{e}^{\bar{\lambda}_P^{(1)}x}\bar{\xi}_{P1}^{(1)} & \dots \mathrm{e}^{\bar{\lambda}_P^{(4)}x}\bar{\xi}_{P1}^{(4)} \\ \vdots & \dots & \vdots \\ \mathrm{e}^{\bar{\lambda}_P^{(1)}x}\bar{\xi}_{P4}^{(1)} & \dots \mathrm{e}^{\bar{\lambda}_P^{(4)}x}\bar{\xi}_{P4}^{(4)} \end{bmatrix} \begin{bmatrix} \bar{C}_P^{(1)} \\ \vdots \\ \bar{C}_P^{(4)} \end{bmatrix} \\ &= \bar{C}_P^{(1)}[\phi_1(x)] + \dots + \bar{C}_P^{(4)}[\phi_4(x)] \end{aligned} \tag{35}$$

with the constants specified by the boundary conditions. The matrix $\boldsymbol{\Phi}(x)$ of fundamental solution of (29b) is formed by the vectors $[\phi_i(x)]$.

The particular solution to the non-homogeneous equation (29b) can be written in the form:

$$\mathbf{z}_P^{(p)}(x) = \boldsymbol{\Phi}(x)\int \boldsymbol{\Phi}^{-1}(x)\mathbf{F}(x)\mathrm{d}x, \tag{36}$$

and thus the general solution of (29b) is:

$$\mathbf{z}_P = \mathbf{z}_P^{(g)}(x) + \mathbf{z}_P^{(p)}(x) = \boldsymbol{\Phi}(x)\bar{\mathbf{C}}_P^{(i)} + \boldsymbol{\Phi}(x)\int \boldsymbol{\Phi}^{-1}(x)\mathbf{F}(x)\mathrm{d}x, \tag{37}$$

for $i = 1, \dots, 4$, or, in the matrix form:

$$\mathbf{z}_P = \begin{bmatrix} \mathrm{e}^{\bar{\lambda}_P^{(1)}x}\bar{\xi}_{P1}^{(1)} & \dots & \mathrm{e}^{\bar{\lambda}_P^{(4)}x}\bar{\xi}_{P1}^{(4)} \\ \vdots & \dots & \vdots \\ \mathrm{e}^{\bar{\lambda}_P^{(1)}x}\bar{\xi}_{P4}^{(1)} & \dots & \mathrm{e}^{\bar{\lambda}_P^{(4)}x}\bar{\xi}_{P4}^{(4)} \end{bmatrix} \begin{bmatrix} \bar{C}_P^{(1)} \\ \vdots \\ \bar{C}_P^{(4)} \end{bmatrix} + \mathbf{J}, \tag{38}$$

where vector **J** represents the integral term of (37). With the use of (32) and (38), the system of the boundary conditions (20) can be reduced to the form:

$$\mathbf{K}\bar{\mathbf{C}} = \mathbf{L}, \tag{39}$$

where **K** is the 8×8 matrix presented in Appendix, and $\bar{\mathbf{C}}$ is a vector of unknown constants. Equation (39) has non-trivial solutions, unless its determinant is equal to zero; the solution, that is the vector of constants $\bar{\mathbf{C}}$, can be obtained by Gaussian elimination. The solution of (29) is therefore completely determined, and the conjugate variables can be found in the domains F (subinterval $0 \le x \le x_1$) and P (subinterval $x_1 \le x \le \frac{a}{2}$). The set of regular and conjugate variables in F allows us to find H_1.

The micro-geometry of the focusing structure is thus specified by the following procedure. We first assume that $m = 0$ on the entire interval $[0, x_1)$, solve the combined system (14), (19) with the boundary conditions (17), (20), and calculate the value of H_1 on the same interval of x.

If $H_1 < 0$ on this interval, the solution is achieved by the use of material D_2 in the entire domain F. If H_1 is negative, say, for $x \in [0, x_2)$, $x_2 < x_1$, and positive for $x \in (x_2, x_1)$, then we change the control m on the latter subinterval, assuming that

$$m = \begin{cases} 0, & 0 \le x \le x_2 \le x_1 \\ 1, & x_2 \le x \le x_1 \end{cases} . \tag{40}$$

We again solve the combined system, etc. After N iterations, we evaluate the set of switching points $x_2, x_3, \ldots$. If this set reveals the tendency to become dense on some subinterval of $[0, x_1)$, then on this subinterval we arrange a singular range, and beyond this subinterval we place the pure original materials distributed in accordance with the information revealed through the preceding iterations. The ultimate material deployment involves parts occupied by pure materials 1 and 2, as well as the parts filled by the laminar composite assembled of these materials as of original constituents. The volume fraction $m(x)$ will become a variable characteristic of such a composite; its variability reflects the special design features generated by the external factors, such as the permittivity of the processed material and the relative dimensions of the system.

5. Numerical illustrations: lossless layer

The general scheme outlined above can be reduced to a special case when the material in the domain P in a rectangular applicator is assumed to be lossless. In this case, the requirement for the controlling material to be lossy (8)–(10) does not hold. We pose the following practical question: what should be the dielectric constant $\epsilon_F = \epsilon'_F$ of the uniform dielectric occupying the left and right domains F so that the relevant electric field E_y within the domain P becomes uniform?

Since the materials in P and F are now lossless, the propagation factor γ is equal to the phase constant β. Let us consider two configurations of the controlling dielectrics occupying the lateral spaces either completely, or in part.

5.1. P AND F IN CONTACT

The geometry of this problem is represented by Figure 2. The analysis of this problem shows that:

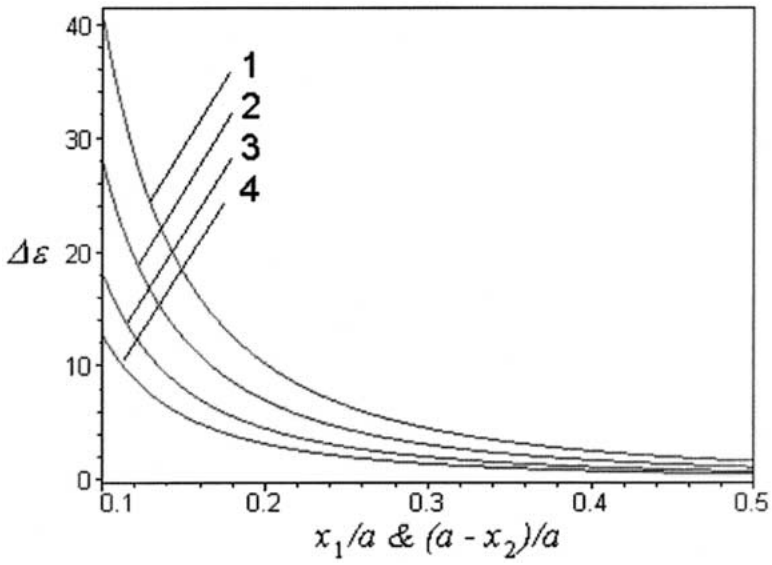

Figure 4. Applicator in Figure 2: permittivity increment (41) versus normalized thickness of the controlling layer at 2·45 GHz for the standard waveguides WR187/WG12 ($a = 48$ mm) (1), WR229/WG11A ($a = 58$ mm) (2), WR284/WG10 ($a = 72$ mm) (3), and WR340/WG9A ($a = 86$ mm) (4).

(i) the uniform field E_y within P is maintained if the effective permittivity ϵ_F of the controlling layers in each of the F subdomains $x \in (0, x_1)$ and $x \in (x_2, a)$ are uniform; thus, no composite structures arise there;

(ii) the value of ϵ_F exceeds ϵ_P, and the permittivity increment $\Delta\epsilon_F = \epsilon_F - \epsilon_P$ depends on the operating frequency f and location of the processed material according to the formula:

$$\Delta\epsilon_{F1,2} = \left(\frac{h}{\omega}\right)^2, \tag{41}$$

where h is determined by

$$h = \begin{cases} \dfrac{\pi}{2x_1}, & \text{for domain } F_1, \\ \dfrac{\pi}{2(a - x_2)}, & \text{for domain } F_2. \end{cases} \tag{42}$$

In a symmetric case, Figure 4 illustrates the dependence between the relative permittivity increment $\Delta\epsilon = \Delta\epsilon_F/\epsilon_0$, where ϵ_0 is the permittivity of a vacuum, and the normalized widths of the controlling layers. One may see that the thicker is the processed material in P, the larger value of the controlling material in F is required to guarantee the uniform field distribution.

The electric field within the intervals specified in (4) has been calculated without the additional requirement (6) and for the fixed value $\epsilon_P = 5{\cdot}5$ and variable values ϵ_F. A similar analysis (though applied for $\epsilon_F < \epsilon_P$) can be found in [24]. The graphs presented in Figure 5 show that the field becomes uniform for $x\epsilon(x_1, x_2)$ if $\epsilon_F = 6{\cdot}6$ which is consistent with the value computed from (8).

This illustration shows that the practical implementation of control over the electric field may be associated with materials D_1 and D_2 possessing high values of the real part of their dielectric constants. For example, ϵ'_P of the typical microwavable food products is known to be between 30 and 70 [28, Chapter 5, Appendix 3]. At the same time, as follows from (ii) and

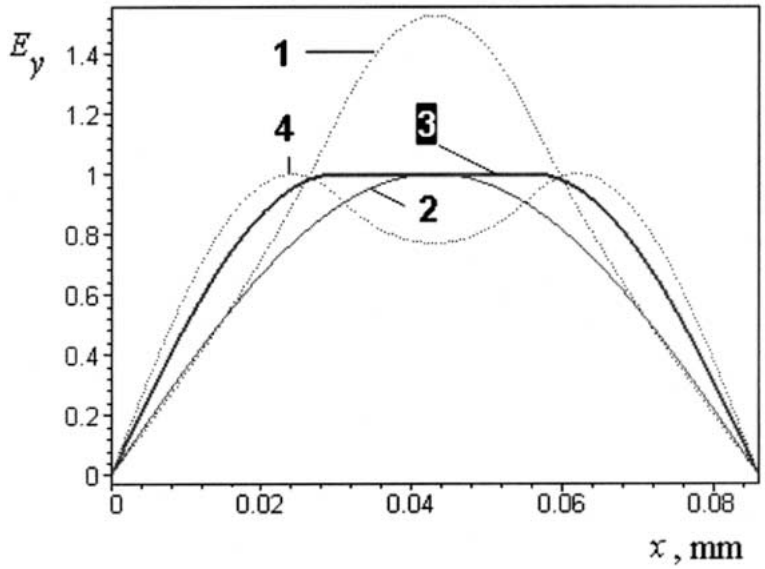

Figure 5. Magnitude of the relative electric field of the dominant TE_{10} mode in the WR340/WG9A waveguide ($a = 86$ mm) with $\epsilon_P = 5{\cdot}5$ and $\epsilon_F = 4$ (1), 5·5 (2), 6·6 (3), 8 (4).

(41), ϵ'_F of the efficient controlling materials is expected to be larger than that of the food. If the thickness of material in domain F is supposed to be small, this leads to further increase of its dielectric constant. Numerical estimate suggests that the required materials may possess ϵ'_F about 40–150 and ϵ''_F about 0·0005–0·005.

5.2. P AND F SEPARATED

The previous example can be extended to cover a practically significant case when there is no direct contact between the material $[x \in (x_1, x_2)]$ and the controlling layers $[x \in (0, x_{10})$ and $x \in (x_{20}, a), x_{10} < x_1, x_{20} > x_2]$, like shown in Figure 6. Instead, they are separated by an empty space (or the space filled by the third material), and the relevant control action is implemented by a due choice of ϵ_F.

The field representation (2) remains the same along with the Helmholtz's equation (3). Assuming that the permittivity is equal to ϵ_0 in the space between the focusing and processed material, we observe that the uniform field in the interval (x_1, x_2) is given by (6), and the minimal requirement has the same form (7). The analysis of this problem shows that:

(i) the uniform field E_y within P is maintained if the effective permittivities ϵ_F in the x-direction are uniform in each of the F-subdomains occupied by controlling layers;

(ii) the values of ϵ_{F1} and ϵ_{F2} exceed ϵ_P and the permittivity increment is determined by (41), but, instead of (42), h is defined as the root of the equations

$$\begin{aligned} \sqrt{h}\cot\left(\sqrt{h}x_{10}\right) &= -\sqrt{|h_0|}\tanh\left[\sqrt{|h_0|}(x_1 - x_{10})\right], \text{ for domain } F_1, \\ \sqrt{h}\cot\left[\sqrt{h}(a - x_{20})\right] &= -\sqrt{|h_0|}\tanh\left[\sqrt{|h_0|}(x_{20} - x_2)\right], \text{ for domain } F_2. \end{aligned} \tag{43}$$

where $h_0 = \omega^2(\epsilon_0 - \epsilon_F)$. The curves illustrating the dependence between the increment $\Delta\epsilon$ and the normalized widths of the controlling layers are shown in Figure 7. The curves come

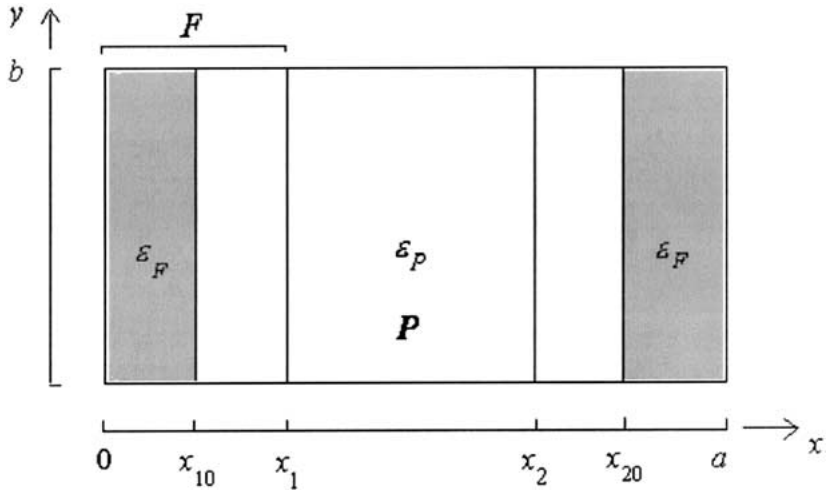

Figure 6. Cross-section of a rectangular traveling wave applicator with focusing (F) and processed (P) materials separated by air gap.

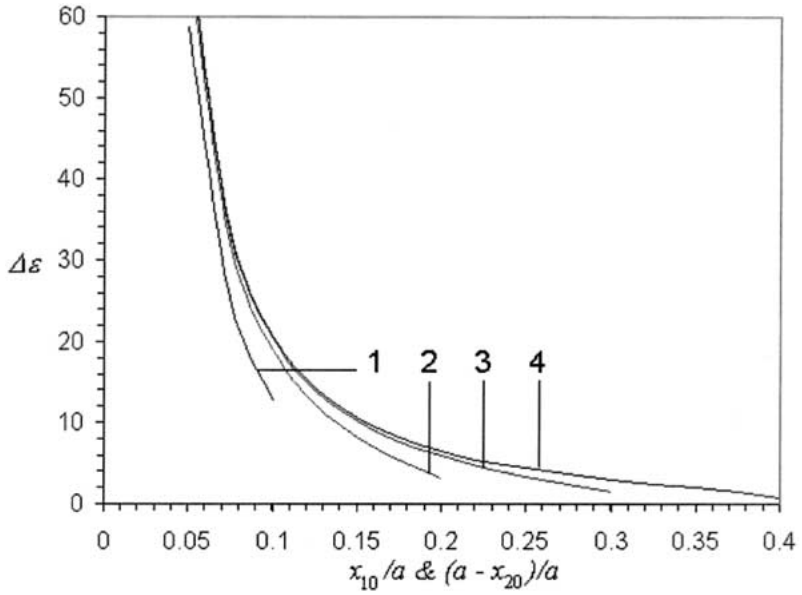

Figure 7. Applicator in Figure 6: permittivity increment (41) versus normalized thickness of the controlling layer at 2·45 GHz for various sizes of the air gap $(x_1 - x_{10})/a$ & $(x_{20} - x_2)/a = 0{\cdot}1$ (1), 0·2 (2), 0·3 (3), and 0·4 (4).

to the points $x_{10}/a = x_1/a$, or $(a - x_{20})/a = (a - x_2)/a$ (lower points on each curve) corresponding to the case of no gap between the controlling layers and the processed material. It is obvious that the air gap produces a notable increase of the permittivity increment required to make the field in P uniform.

6. Conclusion

This paper gives a design procedure for the focusing dielectric structure that creates a uniform electric field within a layer of processed material in a rectangular applicator. Presented for

the dominant (TE_{10}) mode and the centered E-plane dielectric layer, the procedure can be expanded for the higher modes and more complex configuration of the processed material.

The dominant mode is considered in the supposition that a single-mode regime is maintained in a rectangular applicator. However, the multimode wave propagation may generally emerge in the waveguides filled with dielectric materials. The single-mode wave propagation will take place in the structures shown in Figures 2 and 6 provided that the dielectric constants of both processed and controlling materials are not too large.

For larger values of ϵ'_P and ϵ'_F, the multimode propagation may occur with some finite number of higher modes existing at one time. The analysis demonstrated above for a dominant mode may equally be applied in this more complex situation. The procedure will be affected, however, by the presence of additional parameters measuring the relative amplitudes of the traveling modes generating the heat release, and these parameters generally may serve as additional design factors.

The presented analysis suggests that, in order to exclude heating of the controlling material in F, it would be reasonable to agree on some non-uniformity of the field within the processed material in P by preserving the controlling material lossless. The degree of non-uniformity of the field within P in this case is affected by the micro-geometry of the composite structure in F. The permittivity of each component of the efficient controlling material may be higher than the one of the processed material.

Appendix

Matrices in the differential equations (25) and (26) have the following structures:

$$\mathbf{A}_F = \begin{bmatrix} 0 & 1 & 0 & 0 \\ -f_{Fi} & 0 & g_{Fi} & 0 \\ 0 & 0 & 0 & 1 \\ -g_{Fi} & 0 & -f_{Fi} & 0 \end{bmatrix}, \quad \mathbf{A}_P = \begin{bmatrix} 0 & 1 & 0 & 0 \\ -f_P & 0 & g_P & 0 \\ 0 & 0 & 0 & 1 \\ -g_P & 0 & -f_P & 0 \end{bmatrix},$$

$$\mathbf{D}_F = \begin{bmatrix} 0 & f_{Fi} & 0 & g_{Fi} \\ -1 & 0 & 0 & 0 \\ 0 & -g_{Fi} & 0 & f_{Fi} \\ 0 & 0 & -1 & 0 \end{bmatrix}, \quad \mathbf{D}_P = \begin{bmatrix} 0 & f_P & 0 & g_P \\ -1 & 0 & 0 & 0 \\ 0 & -g_P & 0 & f_P \\ 0 & 0 & -1 & 0 \end{bmatrix}.$$

Matrices in the systems of the boundary conditions (28) and (38) are represented as follows:

$$\mathbf{B}=\begin{bmatrix}
\xi_{F1}^{(1)} & \xi_{F1}^{(2)} & \xi_{F1}^{(3)} & \xi_{F1}^{(4)} & 0 & 0 & 0 & 0\\
\xi_{F3}^{(1)} & \xi_{F3}^{(2)} & \xi_{F3}^{(3)} & \xi_{F3}^{(4)} & 0 & 0 & 0 & 0\\
e^{\lambda_F^{(1)}x_1}\xi_{F1}^{(1)} & e^{\lambda_F^{(2)}x_1}\xi_{F1}^{(2)} & e^{\lambda_F^{(3)}x_1}\xi_{F1}^{(3)} & e^{\lambda_F^{(4)}x_1}\xi_{F1}^{(4)} & -e^{\lambda_P^{(1)}x_1}\xi_{P1}^{(1)} & -e^{\lambda_P^{(2)}x_1}\xi_{P1}^{(2)} & -e^{\lambda_P^{(3)}x_1}\xi_{P1}^{(3)} & -e^{\lambda_P^{(4)}x_1}\xi_{P1}^{(4)}\\
e^{\lambda_F^{(1)}x_1}\xi_{F2}^{(1)} & e^{\lambda_F^{(2)}x_1}\xi_{F2}^{(2)} & e^{\lambda_F^{(3)}x_1}\xi_{F2}^{(3)} & e^{\lambda_F^{(4)}x_1}\xi_{F2}^{(4)} & -e^{\lambda_P^{(1)}x_1}\xi_{P2}^{(1)} & -e^{\lambda_P^{(2)}x_1}\xi_{P2}^{(2)} & -e^{\lambda_P^{(3)}x_1}\xi_{P2}^{(3)} & -e^{\lambda_P^{(4)}x_1}\xi_{P2}^{(4)}\\
e^{\lambda_F^{(1)}x_1}\xi_{F3}^{(1)} & e^{\lambda_F^{(2)}x_1}\xi_{F3}^{(2)} & e^{\lambda_F^{(3)}x_1}\xi_{F3}^{(3)} & e^{\lambda_F^{(4)}x_1}\xi_{F3}^{(4)} & -e^{\lambda_P^{(1)}x_1}\xi_{P3}^{(1)} & -e^{\lambda_P^{(2)}x_1}\xi_{P3}^{(2)} & -e^{\lambda_P^{(3)}x_1}\xi_{P3}^{(3)} & -e^{\lambda_P^{(4)}x_1}\xi_{P3}^{(4)}\\
e^{\lambda_F^{(1)}x_1}\xi_{F4}^{(1)} & e^{\lambda_F^{(2)}x_1}\xi_{F4}^{(2)} & e^{\lambda_F^{(3)}x_1}\xi_{F4}^{(3)} & e^{\lambda_F^{(4)}x_1}\xi_{F4}^{(4)} & -e^{\lambda_P^{(1)}x_1}\xi_{P4}^{(1)} & -e^{\lambda_P^{(2)}x_1}\xi_{P4}^{(2)} & -e^{\lambda_P^{(3)}x_1}\xi_{P4}^{(3)} & -e^{\lambda_P^{(4)}x_1}\xi_{P4}^{(4)}\\
0 & 0 & 0 & 0 & e^{\lambda_P^{(1)}\frac{a}{2}}\xi_{P2}^{(1)} & e^{\lambda_P^{(2)}\frac{a}{2}}\xi_{P2}^{(2)} & e^{\lambda_P^{(3)}\frac{a}{2}}\xi_{P2}^{(3)} & e^{\lambda_P^{(4)}\frac{a}{2}}\xi_{P2}^{(4)}\\
0 & 0 & 0 & 0 & e^{\lambda_P^{(1)}\frac{a}{2}}\xi_{P4}^{(1)} & e^{\lambda_P^{(2)}\frac{a}{2}}\xi_{P4}^{(2)} & e^{\lambda_P^{(3)}\frac{a}{2}}\xi_{P4}^{(3)} & e^{\lambda_P^{(4)}\frac{a}{2}}\xi_{P4}^{(4)}
\end{bmatrix}$$

$$\mathbf{K}=\begin{bmatrix}
\bar{\xi}_{F2}^{(1)} & \bar{\xi}_{F2}^{(2)} & \bar{\xi}_{F2}^{(3)} & \bar{\xi}_{F2}^{(4)} & 0 & 0 & 0 & 0\\
\bar{\xi}_{F4}^{(1)} & \bar{\xi}_{F4}^{(2)} & \bar{\xi}_{F4}^{(3)} & \bar{\xi}_{F4}^{(4)} & 0 & 0 & 0 & 0\\
e^{\bar{\lambda}_F^{(1)}x_1}\bar{\xi}_{F1}^{(1)} & e^{\bar{\lambda}_F^{(2)}x_1}\bar{\xi}_{F1}^{(2)} & e^{\bar{\lambda}_F^{(3)}x_1}\bar{\xi}_{F1}^{(3)} & e^{\bar{\lambda}_F^{(4)}x_1}\bar{\xi}_{F1}^{(4)} & -e^{\bar{\lambda}_P^{(1)}x_1}\bar{\xi}_{P1}^{(1)} & -e^{\bar{\lambda}_P^{(2)}x_1}\bar{\xi}_{P1}^{(2)} & -e^{\bar{\lambda}_P^{(3)}x_1}\bar{\xi}_{P1}^{(3)} & -e^{\bar{\lambda}_P^{(4)}x_1}\bar{\xi}_{P1}^{(4)}\\
e^{\bar{\lambda}_F^{(1)}x_1}\bar{\xi}_{F2}^{(1)} & e^{\bar{\lambda}_F^{(2)}x_1}\bar{\xi}_{F2}^{(2)} & e^{\bar{\lambda}_F^{(3)}x_1}\bar{\xi}_{F2}^{(3)} & e^{\bar{\lambda}_F^{(4)}x_1}\bar{\xi}_{F2}^{(4)} & -e^{\bar{\lambda}_P^{(1)}x_1}\bar{\xi}_{P2}^{(1)} & -e^{\bar{\lambda}_P^{(2)}x_1}\bar{\xi}_{P2}^{(2)} & -e^{\bar{\lambda}_P^{(3)}x_1}\bar{\xi}_{P2}^{(3)} & -e^{\bar{\lambda}_P^{(4)}x_1}\bar{\xi}_{P2}^{(4)}\\
e^{\bar{\lambda}_F^{(1)}x_1}\bar{\xi}_{F3}^{(1)} & e^{\bar{\lambda}_F^{(2)}x_1}\bar{\xi}_{F3}^{(2)} & e^{\bar{\lambda}_F^{(3)}x_1}\bar{\xi}_{F3}^{(3)} & e^{\bar{\lambda}_F^{(4)}x_1}\bar{\xi}_{F3}^{(4)} & -e^{\bar{\lambda}_P^{(1)}x_1}\bar{\xi}_{P3}^{(1)} & -e^{\bar{\lambda}_P^{(2)}x_1}\bar{\xi}_{P3}^{(2)} & -e^{\bar{\lambda}_P^{(3)}x_1}\bar{\xi}_{P3}^{(3)} & -e^{\bar{\lambda}_P^{(4)}x_1}\bar{\xi}_{P3}^{(4)}\\
e^{\bar{\lambda}_F^{(1)}x_1}\bar{\xi}_{F4}^{(1)} & e^{\bar{\lambda}_F^{(2)}x_1}\bar{\xi}_{F4}^{(2)} & e^{\bar{\lambda}_F^{(3)}x_1}\bar{\xi}_{F4}^{(3)} & e^{\bar{\lambda}_F^{(4)}x_1}\bar{\xi}_{F4}^{(4)} & -e^{\bar{\lambda}_P^{(1)}x_1}\bar{\xi}_{P4}^{(1)} & -e^{\bar{\lambda}_P^{(2)}x_1}\bar{\xi}_{P4}^{(2)} & -e^{\bar{\lambda}_P^{(3)}x_1}\bar{\xi}_{P4}^{(3)} & -e^{\bar{\lambda}_P^{(4)}x_1}\bar{\xi}_{P4}^{(4)}\\
0 & 0 & 0 & 0 & e^{\bar{\lambda}_P^{(1)}\frac{a}{2}}\bar{\xi}_{P1}^{(1)} & e^{\bar{\lambda}_P^{(2)}\frac{a}{2}}\bar{\xi}_{P1}^{(2)} & e^{\bar{\lambda}_P^{(3)}\frac{a}{2}}\bar{\xi}_{P1}^{(3)} & e^{\bar{\lambda}_P^{(4)}\frac{a}{2}}\bar{\xi}_{P1}^{(4)}\\
0 & 0 & 0 & 0 & e^{\bar{\lambda}_P^{(1)}\frac{a}{2}}\bar{\xi}_{P3}^{(1)} & e^{\bar{\lambda}_P^{(2)}\frac{a}{2}}\bar{\xi}_{P3}^{(2)} & e^{\bar{\lambda}_P^{(3)}\frac{a}{2}}\bar{\xi}_{P3}^{(3)} & e^{\bar{\lambda}_P^{(4)}\frac{a}{2}}\bar{\xi}_{P3}^{(4)}
\end{bmatrix}$$

Acknowledgements

This work was supported in part by NSF-NATO Grant No. DGE-9617552, and by EPRI under Contract No. GC-111954.

References

1. J. Thuery, *Microwaves: Industrial, Scientific, and Medical Applications*, Boston-London: Artech House (1992) 670 pp.
2. *Microwave Processing of Materials*, National Research Council, Publication NMAB-473, Washington, DC (1994) 550 pp.
3. J. A. McCormick, Historical and recent attempts to solve microwave heating problems with packaging. *Microwave World* 13 (1992) 17–20.
4. G. J. Vogt, A. Regan, *et al.*, Microwave process control through a traveling wave tube source. *Microwave Processing of Materials V MRS Symp Proc.* 430 (1996) 513–518.
5. A. C. Johnson, R. J. Lauf and A. D. Surrett, Effect of bandwidth on uniformity of energy distribution in a multimode cavity. *Proc. 29th Microwave Power Symp. Chicago, IL, July 1994* 160–163.
6. T. V. Chow Ting Chan and H. C. Reader, Modelling of modes and perspectives on multiple feeds in microwave ovens. *J. Microwave Power & Electromagnetic Energy* 31 (1996) 238–250.
7. R. G. Heeren and J. R. Baird, An inhomogeneously filled rectangular waveguide capable of supporting TEM propagation. *IEEE Trans. Microwave Theory and Techniques* 19 (1971) 884–885.
8. A. L. VanKoughnett and W. Wyslouzil, A waveguide TEM mode exposure chamber. *J. Microwave Power & Electromagnetic Energy* 7 (1972) 381–383.
9. J. T. Bernhard and W. T. Joines, Dielectric slab-loaded resonant cavity for applications requiring enhanced field uniformity. *IEEE Trans. Microwave Theory and Techniques* 44 (1996) 457–460.

10. G. Kantor and D. M. Witters, A 2450 MHz slab-loaded direct contact applicator with choke. *1980 IEEE MTT-S International Microwave Symp. Digest* (1980) 355–357.
11. V. A. Kolomeytsev and V. V. Yakovlev, Family of operating chambers for microwave thermal processing of dielectric mateirials. *Proc. 28th Microwave Power Symp., Montreal, Canada* (1993) 181–186.
12. L. Setti, M. A. Audhuy-Peaudecerf and S. Lefeuvre, Model of a microwave oven containing a metal grid. *Proc. 5th Conf. Microwave & HF Heating, Cambridge, U.K., Sept. 1995* B1.1–B1.4.
13. J. Chang and M. Brodwin, A new applicator for efficient uniform heating using a circular cylindrical geometry. *J. Microwave Power & Electromagnetic Energy* 28 (1993) 32–40.
14. C. Buffler and P. Risman, A new 915 MH low power generator for materials testing utilizing an evanescent mode cavity. In: M. F. Iskander *et al.* (eds.), *Microwave Processing of Materials V, MRS Symp Proc.* 430 (1996) 85–92.
15. D. Dibben and A. C. Metaxas, Frequency domain vs. time domain finite element methods for calculation of fields in multimode cavities. *IEEE Trans. Magn.* 33 (1997) 1468–1471.
16. H. Zhao and I. W. Turner, An analysis of the finite-difference time-domain method for modeling the microwave heating of dielectric materials within a three-dimensional cavity systems. *J. Microwave Power & Electromagnetic Energy* 31 (1996) 199–214.
17. M. Sundberg, P. Kildal and T. Ohlsson, Moment method analysis of a microwave tunnel oven. *J. Microwave Power & Electromagnetic Energy* 33 (1998) 36–48.
18. G. Eves and V. V. Yakovlev, Analysis of operational regimes of a high power water load. *J. Microwave Power & Electromagnetic Energy* 37 (2002) (to be published).
19. M. Sundberg, Microwave modeling - from analysis to synthesis. *Microwave World* 17 (March 1996) 19–22.
20. J. Saa, A. A. Alonso and J. R. Banga, Optimal control of microwave heating using mathematical models of medium complexity. *Proc. of ACoFoP IV (Automatic Control of Food and Biological Processes), Göteborg, Sweden Sept. 21–23, 1998*.
21. K. A. Lurie, *Applied Optimal Control of Distributed Systems*, N.Y.: Plenum (1993) 499 pp.
22. R. Formisano, R. Martone, and F. Villone, A Lagrangian approach to shape inverse electromagnetic problems. *IEEE Trans. Magn.* 32 (1996) 1314–1317.
23. J. Starzynsky, S. Wincenciak and J. Korytkowski, FAT: shape optimization software for electromagnetics. *Intern. J. Computation and Mathematics in Electrical and Electronic Engng* 19 (2000) 657–663.
24. L. Outifa, M. Delmotte and H. Jullien, Dielectric and geometric dependence of electric field and power distribution in a waveguide heterogeneously filled with lossy dielectrics. *IEEE Trans. Microwave Theory and Tech.* 45 (1997) 1154–1161.
25. A. Calmels, D. Stuerga, *et al.*, Modeling propagation in high-power microwave devices. *Microwave & Optical Technology Letters* 21 (1999) 477–482.
26. J. Yoo, N. Kikuchi and J. L. Volakis, Structural optimization in magnetic devices by the homogenization design method. *IEEE Trans. Magn.* 36 (2000) 574–580.
27. C. S. Koh and S. Y. Hahn, A continuum approach in shape design sensitivity analysis of magnetostatic problems using the boundary element method. *IEEE Thans. Magn.* 29 (1993) 1771–1774.
28. C. R. Buffler, *Microwave Cooking and Processing. Engineering Fundamentals for the Food Scientist*, N.Y.: An AVI Book (1993) 169 pp.